OFDM Receiver Using Deep Learning: Redundancy Issues

Marcele O. K. Mendonça and Paulo S. R. Diniz
SMT - Signals, Multimedia, and Telecommunications Lab.
Universidade Federal do Rio de Janeiro, DEL/Poli & PEE/COPPE/UFRJ
P.O. Box 68504, Rio de Janeiro, RJ, 21941-972, Brazil
{diniz, marcele.kuhfuss}@smt.ufrj.br

***Abstract*—To combat the inter-symbol interference (ISI) and the inter-block interference (IBI) caused by multi-path fading in orthogonal frequency-division multiplexing (OFDM) systems, it is usually recommended employing a cyclic prefix (CP) with length equal to the channel order. In some practical cases, however, the channel order is not exactly known. Looking for a balance between a full-sized CP and its absence, we investigate the redundancy issues and propose a minimum redundancy OFDM receiver using deep-learning (DL) tools. In this way, we can benefit from an improved reception performance, when compared with CP-free case, and also a better spectrum utilization when compared with the CP-OFDM case. Moreover, compared with the CP-free case, improved performance can be obtained even when the channel order is not available. Simulation results indicate that a good BER level can be achieved and the proposed technique can also be applied in other DL-based receivers.**

***Index Terms*—deep-learning, channel-estimation, symbol-detection, OFDM, minimum-redundancy**

I. Introduction

The effectiveness of orthogonal frequency-division multiplexing (OFDM) systems when dealing with multi-path fading is well-known in the wireless communications field. At the cost of extra bandwidth, OFDM is capable of combating inter-symbol interference (ISI) and inter-block interference (IBI) caused by the multiple delayed versions of the transmitted signal [1]. The number of redundant elements L, also known as cyclic prefix (CP), should be at least equal to the channel order which is related to the maximum delay spread of the channel [2]. In this way, the linear convolution of the physical channel is converted into circular convolution, eliminating the intersymbol interference and simplifying the receiver. Nevertheless, if the spectrum efficiency is an issue, the CP-free OFDM system is an attractive alternative [3] as long as a proper design for the transceiver is provided. On the other hand, it is known that the required redundancy can be reduced to $L/2$ via efficient channel equalization [4], [5] in the case of zero padding (ZP) OFDM. This solution requires the minimum amount of redundancy allowing a zero-forcing (ZF) equalization [6], [7]. ZF solution is not usually discussed for CP-OFDM with insufficient redundancy, but recent learning methods might enhance the performance and ease the reception.

Due to the enormous success of deep learning (DL) in many fields, recent methods using deep neural networks (DNNs) in wireless communications [3], [8]–[11] have been proposed. Choosing a deep model represents the belief that the system we want to learn should involve the composition of several simpler systems [12]. Indeed, the reception of an OFDM system is composed of several blocks which can be modeled by DNNs [8]. However, more control can be obtained by exploiting the expert knowledge in wireless communications and breaking, for example, a single DNN in two [3], [9]. In this paper, we propose a two-block DL-based OFDM reception operating with reduced redundancy, that is, our work provides the answer of how to would perform a solution lying between a CP-free and CP-OFDM. The results demonstrate that we can benefit from an improved reception performance as well as achieving a better spectrum utilization.

The paper is organized as follows. The considered system model is defined in section II. Section III introduces the proposed reception for an OFDM with minimum redundancy. In section IV, the proposed method is evaluated via simulation results. Section V includes some concluding remarks.

II. System Model

The considered OFDM system is illustrated in Figure 1. At the transmitter side, the input binary data $\mathbf{b} = [\mathrm{b}_1, \mathrm{b}_2, \cdots, \mathrm{b}_B]^{\mathrm{T}}$ are generated. The input symbols are generated from the M-ary quadrature amplitude modulation (M-QAM) and converted to a parallel data stream $\boldsymbol{x} \in \mathbb{C}^{N\times 1}$. The N-point inverse fast Fourier transform (IFFT) is then employed to convert the signal from the frequency domain $\boldsymbol{x}$ to the time domain $\mathbf{x}$. The K-length CP is added, resulting in the OFDM signal

$$\mathbf{u} = \mathbf{A}_{\mathrm{CP}}\mathbf{W}_N^{\mathrm{H}}\boldsymbol{x} = \mathbf{A}_{\mathrm{CP}}\mathbf{x}, \tag{1}$$

where

$$\mathbf{A}_{\mathrm{CP}} = \begin{bmatrix} \mathbf{0}_{K\times(N-K)} & \mathbf{I}_K \\ & \mathbf{I}_N \end{bmatrix} \in \mathbb{C}^{S\times N} \tag{2}$$

and $\mathbf{W}_N$ is the unitary $N \times N$ FFT matrix. Then $S = N + K$ sub-carriers are used to transmit the OFDM symbol $\mathbf{u} \in \mathbb{C}^S$.

This study was financed in part by the Coordenação de Aperfeiçoamento de Pessoal de Nível Superior - Brasil (CAPES) - Finance Code 001. This work was also supported by the research councils: CNPq (Conselho Nacional de Desenvolvimento Científico e Tecnológico), and FAPERJ (Fundação de Amparo à Pesquisa do Estado do Rio de Janeiro).

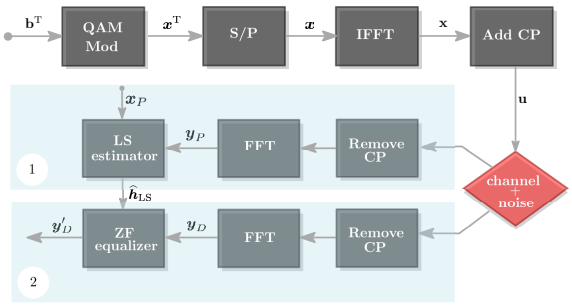

Fig. 1: Basic OFDM system block diagram.

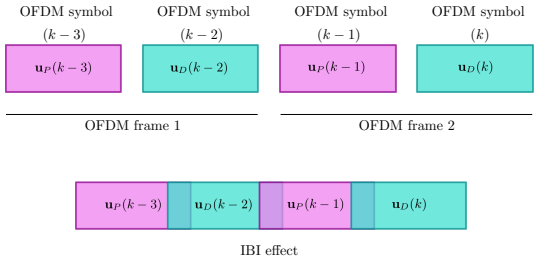

Fig. 2: OFDM frame.

The channel model between transmitter and receiver has the impulse response $\mathbf{h} = [\mathrm{h}(0) \quad \mathrm{h}(1) \quad \cdots \mathrm{h}(\mathrm{L})]^{\mathrm{T}}$. In the z-domain, the pseudo-circulant channel matrix is

$$\begin{aligned}\mathbf{H}(z) = &\begin{bmatrix} \mathrm{h}(0) & 0 & 0 & \cdots & 0 \\ \mathrm{h}(1) & \mathrm{h}(0) & 0 & \cdots & 0 \\ \vdots & \vdots & \vdots & \vdots & \vdots \\ \mathrm{h}(\mathrm{L}) & \mathrm{h}(\mathrm{L}-1) & \ddots & \cdots & 0 \\ 0 & \mathrm{h}(\mathrm{L}) & \cdots & \cdots & 0 \\ \vdots & \vdots & \vdots & \vdots & \vdots \\ 0 & 0 & \mathrm{h}(\mathrm{L}) & \cdots & \mathrm{h}(0) \end{bmatrix}_{S\times S} \\ &+ z^{-1}\begin{bmatrix} 0 & \cdots & 0 & \mathrm{h}(\mathrm{L}) & \cdots & \mathrm{h}(1) \\ & & & & \ddots & \vdots \\ 0 & 0 & \cdots & 0 & & \\ \vdots & \vdots & \vdots & \vdots & \vdots & \mathrm{h}(\mathrm{L}) \\ 0 & 0 & 0 & \cdots & 0 & 0 \\ 0 & 0 & 0 & \cdots & 0 & 0 \\ \vdots & \vdots & \vdots & \vdots & \vdots & \vdots \\ 0 & 0 & 0 & \cdots & 0 & 0 \end{bmatrix}_{S\times S} \\ &= \mathbf{H}_{\mathrm{ISI}} + z^{-1}\mathbf{H}_{\mathrm{IBI}},\end{aligned} \tag{3}$$

in which $\mathbf{H}_{\mathrm{ISI}}$ and $\mathbf{H}_{\mathrm{IBI}}$ represent ISI and IBI effects produced by the wireless channel [2]. By using equation (3), we can express the received signal in the time-domain as

$$\mathbf{y}(k) = \mathbf{H}_{\mathrm{ISI}}\mathbf{u}(k) + \mathbf{H}_{\mathrm{IBI}}\mathbf{u}(k-1) + \mathbf{v}(k), \tag{4}$$

where $\mathbf{v}(k)$ is an additive Gaussian noise vector with zero mean and covariance matrix $\sigma_v^2\mathbf{I}_S$.

We assume that the channel remains approximately constant over the transmission of an OFDM frame. For simplicity, as in [3], [9], an OFDM frame consists of one pilot and one data OFDM symbol. As illustrated in Figure 2, each OFDM symbol suffers from the IBI effect. Following the example in Figure 2, the received data signal at instant k is

$$\mathbf{y}_D(k) = \mathbf{H}_{\mathrm{ISI}}\mathbf{u}_D(k) + \mathbf{H}_{\mathrm{IBI}}\mathbf{u}_P(k-1) + \mathbf{v}(k), \tag{5}$$

where $\mathbf{u}_D$ and $\mathbf{u}_P$ are the data and pilot OFDM symbols, respectively.

As depicted in Figure 1, first the pilot signal $\mathbf{u}_P$ is transmitted using all the S sub-carriers to obtain channel state information (CSI). The receiver removes the CP by multiplying $\mathbf{y}(k)$ by $\mathbf{R}_{\mathrm{CP}} = \begin{bmatrix}\mathbf{0}_{N\times K} & \mathbf{I}_N\end{bmatrix} \in \mathbb{C}^{N\times S}$.

If a CP with sufficient length $K \geq L$ is employed, $\mathbf{R}_{\mathrm{CP}}\mathbf{H}_{\mathrm{IBI}}\mathbf{A}_{\mathrm{CP}} = \mathbf{H}_r = \mathbf{0}_N$ and

$$\mathbf{R}_{\mathrm{CP}}\mathbf{H}_{\mathrm{ISI}}\mathbf{A}_{\mathrm{CP}} = \mathbf{H}_c \in \mathbb{C}^{N\times N} \tag{6}$$

is a circulant matrix. Hence, the matrix equation $\mathbf{y}_P(k) = \mathbf{H}_c\mathbf{x}_P(k)$ can be written as the circular convolution $\mathbf{y}_P(k) = \mathbf{h}_N \circledast \mathbf{x}_P(k)$ in which $\mathbf{h}_N$ is the first column of $\mathbf{H}_c$. The circular convolution is transformed into component-wise multiplication and then we can employ a least-squares (LS) method, to obtain the channel estimate $\widehat{\boldsymbol{h}}_{\mathrm{LS}} \in \mathbb{C}^{N\times 1}$ so that

$$\widehat{h}_{\mathrm{LS}}(n) = \frac{y_P(n)}{x_P(n)} \quad \text{for} \quad n = 1, \cdots N, \tag{7}$$

where $\boldsymbol{x}_P \in \mathbb{C}^{N\times 1}$ and $\boldsymbol{y}_P \in \mathbb{C}^{N\times 1}$ are the transmitted and received pilot signals in the frequency domain. To obtain CSI, we can also employ the linear minimum mean-squared error (LMMSE) channel estimation

$$\begin{aligned}\widehat{\boldsymbol{h}}_{\mathrm{LMMSE}} &= \mathbf{R}_{\boldsymbol{h}_N\widehat{\boldsymbol{h}}_{\mathrm{LS}}}\left(\mathbf{R}_{\boldsymbol{h}_N\boldsymbol{h}_N} + \frac{\sigma_v^2}{E[||\mathbf{x}_P||^2]}\mathbf{I}_N\right)^{-1}\widehat{\boldsymbol{h}}_{\mathrm{LS}} \\ &= \mathbf{W}_{\mathrm{LMMSE}}\widehat{\boldsymbol{h}}_{\mathrm{LS}},\end{aligned} \tag{8}$$

where $\mathbf{R}_{\boldsymbol{h}_N\widehat{\boldsymbol{h}}_{\mathrm{LS}}}$ is the cross-correlation matrix between the true channel vector and channel estimate vector in the frequency domain, $\mathbf{R}_{\boldsymbol{h}_N\boldsymbol{h}_N}$ is the auto-correlation matrix of $\boldsymbol{h}_N$, $E[||\mathbf{x}_P||^2]$ is the energy of the transmitted symbol and $\boldsymbol{h}_N$ is $\mathbf{h}_N$ in the frequency domain. This solution has some practical forms of implementation, see [13].

Then, the data signal $\mathbf{u}_D$ is transmitted, and the previously obtained channel estimate is used to perform frequency domain equalization (FDE)

$$y'_D(n) = \frac{y(n)}{\widehat{h}_{\mathrm{LS}}(n)} \quad \text{for} \quad n = 1, \cdots N, \tag{9}$$

which is equivalent to ZF equalization for $K \geq L$. Finally, the resulting symbols $\boldsymbol{y}'_D$ can be demodulated and the received bits estimated.

III. Minimum Redundancy OFDM Receiver

Let's define the minimum redundancy (MR) OFDM receiver allowing the ZF solution as the one with total redundancy length equal to $L/2$. The proposed MR OFDM receiver is composed of two subnets, as shown in Figure 3.

The first subnet is the same used in [3], [9]. The channel estimator (CE) subnet is responsible for obtaining a refined channel estimate. The second one aims at detecting the received symbols, and it is called symbol detector minimum redundancy (SDMR) subnet.

It should be mentioned that the use of DNN structure here is not a replacement for the traditional channel shortening or other forms to address the redundancy issue.

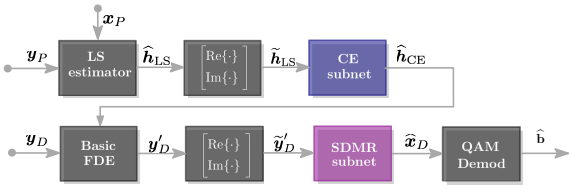

Fig. 3: Proposed minimum redundancy OFDM receiver

A. CE subnet

The CE subnet is first proposed in [9]. Inspired by equation (8), the CE subnet utilizes a two-layer neural network to obtain a refined channel estimation [9], as depicted in Figure 4. The LS estimate described in equation (7) is converted in a real-valued block

$$\widetilde{\boldsymbol{h}}_{\rm LS} = \begin{bmatrix} {\rm Re}\{\widehat{\boldsymbol{h}}_{\rm LS}\} \\ {\rm Im}\{\widehat{\boldsymbol{h}}_{\rm LS}\} \end{bmatrix} \tag{10}$$

and it is used as input of the CE subnet. Moreover, the CE subnet is initialized by the real-valued LMMSE weight matrix

$$\widetilde{\mathbf{W}}_{\rm LMMSE} = \begin{bmatrix} {\rm Re}\{\mathbf{W}_{\rm LMMSE}\} & -{\rm Im}\{\mathbf{W}_{\rm LMMSE}\} \\ {\rm Im}\{\mathbf{W}_{\rm LMMSE}\} & {\rm Re}\{\mathbf{W}_{\rm LMMSE}\} \end{bmatrix} \tag{11}$$

to accelerate the convergence speed. As in [9], we follow the method in [14] to compute the LMMSE matrix $\mathbf{W}_{\rm LMMSE}$ defined in equation (8).

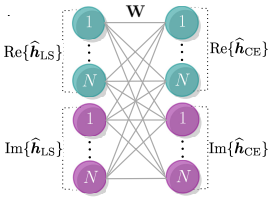

Fig. 4: CE subnet.

The CE subnet is trained by minimizing the mean squared error (MSE) between a noisy version of the actual channel in the frequency domain $\overline{\boldsymbol{h}}_N$ and the prediction $\widehat{\boldsymbol{h}}_{\rm CE}$ by using the adaptive moment estimator (Adam) optimizer. Since obtaining the true channel response is difficult in practice, these training labels are more suitable than the ones used in [3], [9]. We define $\overline{\boldsymbol{h}}_N = \boldsymbol{h}_N + \boldsymbol{v}$, where $\boldsymbol{v}$ is an additive Gaussian noise vector with zero mean and covariance matrix $\sigma_v^2 \mathbf{I}_N$. The learning rate is set to 0.001. The training and testing sets contain 3000 and 1000 samples, respectively. The batch size and epochs are set to 50 and 200, respectively.

B. SDMR-subnet

The proposed symbol detection subnetwork is a DNN with three hidden layers, as illustrated in Figure 5. The hidden layers have as activation function the hyperbolic tangent. In this work, the SDMR subnet utilizes a linear activation function at the output layer. Unlike [8], [9] works concerning bits estimation, the SDMR subnet output layer has been chosen as a linear activation function since it provides a better estimation for the symbols.

We first obtain the frequency domain equalizer solution,

$$y'_D(n) = \frac{y_D(n)}{\widehat{h}_{\rm CE}(n)} \quad \text{for} \quad n = 1, \cdots N, \tag{12}$$

in which $\widehat{\boldsymbol{h}}_{\rm CE}$ is the channel estimate obtained in the CE subnet. Then, the real-valued block version of $\boldsymbol{y}'_D$ is used as input in the SDMR subnet. The output $\widehat{\boldsymbol{x}}$ is then converted to complex vector and it is demodulated to obtain the estimated bits.

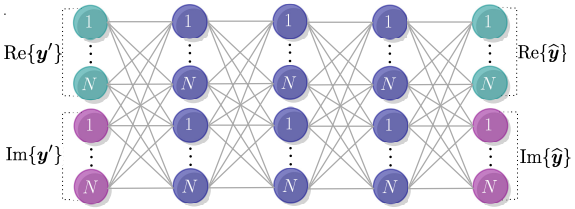

Fig. 5: Proposed SDMR subnet.

An FDE provides a simple technique to mitigate the distortion due to a frequency selective channel. For linear channel model, The use of a cyclic prefix in OFDM with $K \geq L$ not only prevents the IBI but also transforms the linear convolutions into circular convolutions which are equivalent to multiplication in the frequency domain [15]. Consider now using CP with $K = L/2$. In this case, $\mathbf{H}_c$ in equation (6) is no longer circulant, $\mathbf{H}_r \neq \mathbf{0}_N$ and hence the FDE does not provide the ZF solution. Figures 6 and 7 illustrate the impact on matrices $\mathbf{H}_c$ and $\mathbf{H}_r$ when K is reduced. However, as we employ a DNN after the FDE to detect the symbols, the performance is improved. We can then use a reduced CP length and save some of the subcarriers to transmit information data.

The SDMR subnet is also trained by minimizing the mean squared error (MSE) between the actually transmitted symbol $\boldsymbol{x}$ and the prediction $\widehat{\boldsymbol{x}}$ by using the Adam optimizer. The learning rate is set to 0.0001. The training and testing sets contain 3000 and 1000 samples, respectively. The batch size and epochs are set to 50 and 600, respectively.

IV. Simulation Results

In this section, we consider an OFDM system with $S = N + K = 64$ subcarriers. The input symbols are 16-QAM or 64-QAM samples. The OFDM frame consists of one pilot and one data OFDM symbols. Each OFDM symbol suffers from the IBI effect, as shown in Figure 2. As in [3], [8], [9], the channel is modeled by the wireless world initiative for new radio (WINNER II) [16] under urban scenarios. We also consider a scenario in which a nonlinearity, modeled by the hyperbolic tangent function, is present at the transmitter output. Furthermore, we analyze the case in which the channel order is small when compared with the transmit block size.

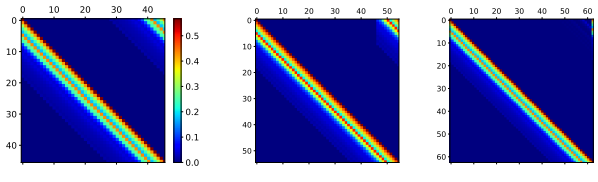

(a) $\mathbf{H}_c$, $K = L$ (b) $\mathbf{H}_c$, $K = L/2$ (c) $\mathbf{H}_c$, $K = 1$

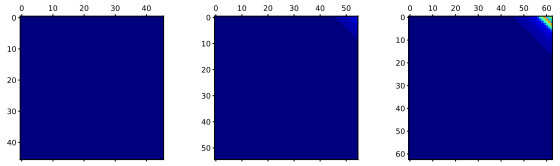

(d) $\mathbf{H}_r$, $K = L$ (e) $\mathbf{H}_r$, $K = L/2$ (f) $\mathbf{H}_r$, $K = 1$

Fig. 6: Illustration of matrices $\mathbf{H}_c$ and $\mathbf{H}_r$ for $S = 64, L = 18$ when K is varied.

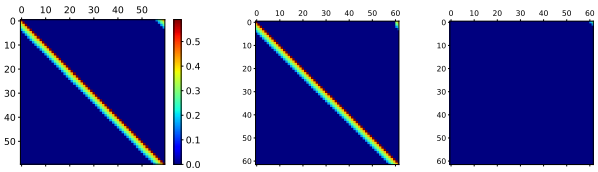

(a) $\mathbf{H}_c$, $K = L$ (b) $\mathbf{H}_c$, $K = L/2$ (c) $\mathbf{H}_r$, $K = L/2$

Fig. 7: Illustration of matrices $\mathbf{H}_c$ and $\mathbf{H}_r$ for $S = 64, L = 4$ when K is varied.

The training procedures for CE and SDMR subnets were specified in subsections III-A and III-B, respectively.

All the simulation results are obtained by averaging $T = 500$ independent runs. The averaged bit error rate (BER) is presented as a function of the signal-to-noise ratio (SNR). The noise variance is varied in order to achieve several values of the SNR, $\rho \in \{5, 40\}$ dB. The methods tested in the simulations are summarized in Table I. The considered methods are presented in more detail in Table II, as well as the main OFDM system. Unfortunately, the methods proposed in [3], [9] are not evaluated in the simulations since the information needed to perform a fair comparison is not available. As shown in Table II, the nonlinearity is not known to the 'Exact_wCP' method when it is present in the transmitter. In this case, 'Exact_wCP' method ignores the nonlinearity and takes into account the exact linear-channel model.

Figure 8 depicts the average BER for an OFDM receiver with a 16-QAM under the linear scenario. The performance of the proposed MR-net with reduced CP is closer to the lower bound, Exact_CP. Moreover, MR-net outperforms the conventional OFDM receiver (LMMSE_wCP). By comparing the proposed method with reduced CP and its CP-free version, we can observe a large gain in performance. This unveils the possibility of applying the minimum redundancy technique with other DNN-based receivers in OFDM.

The proposed method performs quite well under higher modulations schemes like 64-QAM, as illustrated in Figure 9.

TABLE I: OFDM system for SNR, ρ.

OFDM system for SNR, ρ

[Data-set and Training]:
1) Generate the data-set for CE-subnet ($K = L/2$) and CE-subnet ($K = 0$)
2) Train CE-subnet ($K = L/2$) and and CE-subnet ($K = 0$)
3) Generate the data-set for SDMR-subnet ($K = L/2$) using trained CE-subnet ($K = L/2$)
4) Generate the data-set for SDMR-subnet ($K = 0$) using trained CE-subnet ($K = 0$)
5) Train SDMR-subnet ($K = L/2$) and SDMR-subnet ($K = 0$)
Do for $t = 1 : T$ (Each independent run)
  [Pilot phase]:
  Generate pilot signal $\mathbf{u}_P$, where ($K = 0, K = L/2$ or $K = L$)
  If nonlinearity is present:
    $\mathbf{u}_P = \tanh\{\mathbf{u}_P\}$
  end
  Simulate channel impulse response $\mathbf{h}$ and noise $\mathbf{v}$ for given SNR ρ
  Receive pilot symbols $\mathbf{y}_P$ as in equation (4) and estimate channel
  $\widehat{h}_{\mathrm{LS}}(n) = \frac{y_P(n)}{x_P(n)}$ for $n = 1, \cdots N$
  If MR-net_wCP_red:
    Obtain refined estimated channel using CE-subnet ($K = L/2$)
  If LMMSE_wCP:
    $\widehat{\boldsymbol{h}}_{\mathrm{LMMSE}} = \mathbf{R}_{\boldsymbol{h}_N \hat{\boldsymbol{h}}_{\mathrm{LS}}} \left(\mathbf{R}_{\boldsymbol{h}_N \boldsymbol{h}_N} + \frac{\sigma_v^2}{E[||\mathbf{x}_P||^2]} \mathbf{I}_N \right)^{-1} \widehat{\boldsymbol{h}}_{\mathrm{LS}}$
  If CE + ZF_nCP or MR-net_nCP:
    Obtain refined estimated channel using CE-subnet ($K = 0$)
  end
  [Data phase]:
  Generate pilot signal $\mathbf{u}_D$, where ($K = 0, K = L/2$ or $K = L$)
  If nonlinearity is present:
    $\mathbf{u}_D = \tanh\{\mathbf{u}_D\}$
  end
  Receive pilot symbols $\mathbf{y}_D$ and perform equalization
  $y'_D(n) = \frac{y(n)}{\widehat{h}_{\mathrm{LS}}(n)}$ for $n = 1, \cdots N$
  If MR-net_wCP_red:
    Obtain estimated symbol $\widehat{\boldsymbol{x}}'_D$ using SDMR-subnet ($K = L/2$)
  If MR-net_nCP:
    Obtain estimated symbol $\widehat{\boldsymbol{x}}'_D$ using SDMR-subnet ($K = 0$)
  If Exact_wCP:
    $\widehat{x}'_D(n) = \frac{y(n)}{h_N(n)}$ for $n = 1, \cdots N$
  Else:
    $\widehat{\boldsymbol{x}}'_D = \boldsymbol{y}'_D$
  Obtain estimated bits $\widehat{\mathbf{b}}$ by demodulating $\widehat{\boldsymbol{x}}'_D$
  end
end

TABLE II: Methods evaluated in the simulations.

Method	CP length	Channel estimation	Equalization
MR-net_wCP_red	$K = L/2$	CE subnet	ZF+SDMR
LS_wCP_red	$K = L/2$	LS	ZF
LMMSE_wCP	$K = L$	LMMSE	ZF
Exact_wCP	$K = L$	Exact	ZF
CE + ZF_nCP	$K = 0$	CE subnet	ZF
MR-net_nCP	$K = 0$	CE subnet	ZF+SDMR
LS_nCP	$K = 0$	LS	ZF

Figure 10 depicts the average BER for an OFDM system operating with 16-QAM modulation scheme when nonlinearity is present. In this case, the conventional method LMMSE_wCP achieves worse BER levels as the nonlinearity is not known. On the other hand, the performance achieved by the proposed method MR-net remains closer to the lower bound.

Figure 11 depicts the BER results when the channel order is reduced to $L = 4$ and, as in the scenario considered in Figure 9, a nonlinearity is present in the transmitter. In this case, the proposed methods outperform the competing methods, whereas the Exact_wCP shows resilience to the nonlinearity effect applied to the transmitted symbols.

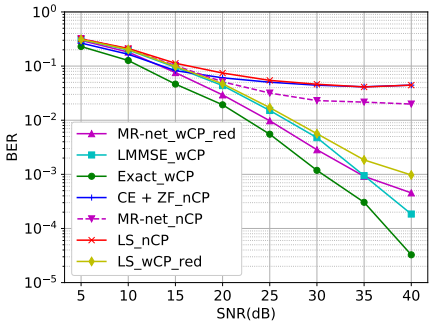

Fig. 8: Average BER for a minimum redundancy OFDM receiver with 16-QAM ($L = 18$).

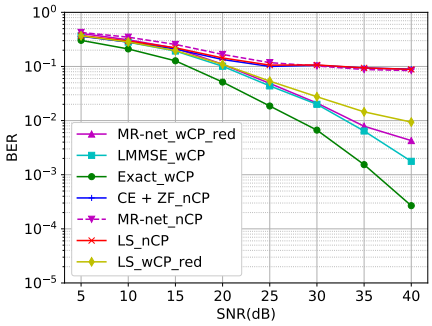

Fig. 9: Average BER for a minimum redundancy OFDM receiver with 64-QAM under linear scenario ($L = 18$).

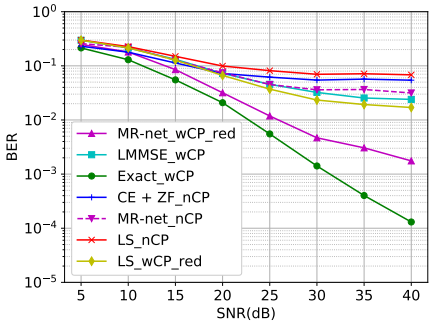

Fig. 10: Average BER for a minimum redundancy OFDM receiver with 16-QAM under nonlinear scenario ($L = 18$).

V. Conclusion

Looking for a balance between improved BER performance and spectrum efficiency, we proposed a minimum redundancy OFDM receiver using two DNNs. The simulation results under linear and nonlinear scenarios indicate that good performance balance can be achieved. Furthermore, other DNN-based OFDM receivers can benefit from the proposed minimum redundancy method.

In the future investigation, we will also address the trade-off between the CP-free scheme and some reduced redundancy solutions in which the redundancy ranges from the channel model order to a single entry.

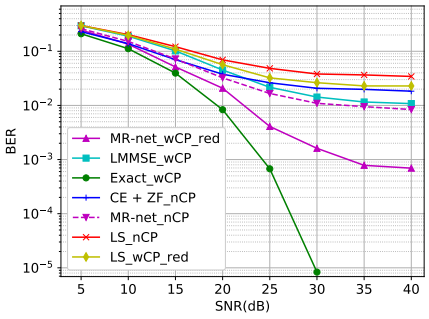

Fig. 11: Average BER for a minimum redundancy OFDM receiver with 16-QAM under nonlinear scenario ($L = 4$).

References

[1] R. Prasad, *OFDM for wireless communications systems*, Artech House Publishers, Boston, 2004.

[2] P. S. R. Diniz, W. A. Martins, and M. V. S. Lima, *Block Transceivers: OFDM and Beyond*, Morgan & Claypool Publishers, USA, 2012.

[3] J. Zhang, H. He, C. K. Wen, S. Jin, and G. Y. Li, "Deep learning based on orthogonal approximate message passing for CP-free OFDM," *IEEE International Conference on Acoustics, Speech, and Signal Processing (ICASSP)*, pp. 8414–8418, 2019, Brighton.

[4] Yuan-Pei Lin and See-May Phoong, "Minimum redundancy for ISI free FIR filterbank transceivers," *IEEE Transactions on Signal Processing*, vol. 50, no. 4, pp. 842–853, Apr 2002.

[5] W. A. Martins and P. S. R. Diniz, "Minimum redundancy multicarrier and single-carrier systems based on hartley transforms," *2009 17th European Signal Processing Conference*, pp. 661–665, 2009, Glasgow.

[6] W. A. Martins and P. S. R. Diniz, "Block-based transceivers with minimum redundancy," *IEEE Transactions on Signal Processing*, vol. 58, no. 3, pp. 1321–1333, Mar 2009.

[7] W. A. Martins and P. S. R. Diniz, "LTI transceivers with reduced redundancy," *IEEE Transactions on Signal Processing*, vol. 60, no. 2, pp. 766–780, Feb 2011.

[8] H. Ye, G. Y. Li, and B. H. Juang, "Power of deep learning for channel estimation and signal detection in OFDM systems," *IEEE Wireless Communications Letters*, vol. 7, no. 1, pp. 114–117, Feb 2017.

[9] X. Gao, S. Jin, C. K. Wen, and G. Y. Li, "Comnet: Combination of deep learning and expert knowledge in OFDM receivers," *IEEE Communications Letters*, vol. 22, no. 12, pp. 2627–2630, Dec 2018.

[10] Z. Qin, H. Ye, G. Y. Li, and B. H. F. Juang, "Deep learning in physical layer communications," *IEEE Wireless Communications*, vol. 26, no. 2, pp. 93–99, Apr 2019.

[11] P. Dong, H. Zhang, G. Y. Li, N. NaderiAlizadeh, and I. S. Gaspar, "Deep CNN for wideband Mmwave massive MIMO channel estimation using frequency correlation," *IEEE International Conference on Acoustics, Speech, and Signal Processing (ICASSP)*, pp. 4529–4533, 2019, Brighton.

[12] I. Goodfellow, Y. Bengio, and A. Courville, *Deep learning*, MIT Press, London, England, 2016.

[13] H. He, C.-K Wen, S. Jin, and G. Y. Li, "Model-driven deep learning for MIMO detection," *IEEE Transactions on Signal Processing*, vol. 68, pp. 1702–1715, Feb 2020.

[14] Y. S. Cho, J. Kim, W. Y. Yang, and C. G. Kang, *MIMO-OFDM wireless communications with MATLAB*, John Wiley & Sons, Singapore, 2010.

[15] A. U. Ahmed, S. C. Thompson, and J. R. Zeidler, "Channel estimation and equalization for CE-OFDM in multipath fading channels," *IEEE Military Communications Conference*, pp. 1–7, 2008, San Diego.

[16] J. Meinilä, P. Kyösti, T. Jämsä, and L. Hentilä, "Winner II channel models," *Radio Technologies and Concepts for IMT-Advanced*, pp. 39–92, 2009, Wiley Online Library.